Research Article

Calcium Phosphate Treatment Enhances Osteogenic Differentiation of Porcine Adipose-Derived Stem Cells on Fibrin Scaffolds

Aaron J. Maki[1,3], R. A. Chanaka Rabel[1,2] and Matthew B. Wheeler[1,2,3,4]*

[1]*Department of Animal Sciences, University of Illinois at Urbana-Champaign, Urbana, Illinois, USA*

[2]*Carl R. Woese Institute for Genomic Biology, University of Illinois at Urbana-Champaign, Urbana, Illinois, USA*

[3]*Department of Bioengineering, University of Illinois at Urbana-Champaign, Urbana, Illinois, USA*

[4]*Department of Biomedical and Translational Sciences, Carle-Illinois College of Medicine, University of Illinois at Urbana-Champaign, Urbana, Illinois, USA*

A B S T R A C T

This study was designed to develop a fibrin scaffold for optimum *in vitro* osteogenic differentiation of porcine ASCs. Fibrin scaffolds physically and chemically modified to be stiffer or have higher concentrations of calcium and phosphate ions were hypothesized to enhance osteogenic differentiation compared to control fibrin scaffolds. Treatments during coagulation resulted in six scaffold types for comparison: whole blood controls, red blood cell lysis buffer, calcium chloride, calcium hydrogen phosphate, vacuum, and mechanical compression. Based on the results, fibrin supplemented with granules of calcium hydrogen phosphate ($CaHPO_4$) was determined to be the most suitable formulation of those examined. Using calcium phosphate resulted in a fibrin scaffold that coagulated faster ($p = 0.022$), had a rougher surface, higher stiffness, and desirable properties for practical use during surgical operations and scaffolds used in bone tissue engineering. Further, osteogenic differentiation was enhanced on scaffolds treated with calcium phosphate. In addition, fibrin scaffolds treated with RBC lysis buffer were also stiffer than untreated controls. These results are partly explained by ASC attachment and fibrin polymerization during coagulation.

Introduction

One factor less studied in the bone fracture healing process is the role of the natural polymer, fibrin, which is a primary component of blood clots. Blood contains constituents essential for wound healing, including coagulation cascade enzymes and fibrinogen. In its native form, fibrin exists as a soluble monomer, fibrinogen, which circulates through the cardiovascular system. Upon activation through damage-induced exposure to collagen or other mechanisms, fibrinogen converts to insoluble fibrin under the control of a series of enzymatic steps of the coagulation cascade [1]. These polymerizing fibers crosslink together to form a stiff clot that limits blood loss and acts as a scaffold in the wound repair process.

However, while fibrin provides the initial wound microenvironment for bone fracture repair, some aspects of fibrin clots may present challenges to the success of potential ASC therapies. Two possible limitations of fibrin include its comparatively low stiffness and ion concentrations [2]. For example, trabecular bone is approximately four orders of magnitude stiffer than fibrin [3]. Scaffold stiffness on the order of trabecular bone and the presence of calcium and phosphate ions have both been shown to increase osteoblast differentiation [4]. Therefore, modifications that can stiffen fibrin and reasonably increase its local calcium and phosphate ion concentrations may result in improved outcomes for ASC therapy for bone defects.

*Correspondence to: Matthew B. Wheeler, Ph.D., Professor of Biotechnology and Developmental Biology, Department of Animal Sciences, Carl R. Woese Institute for Genomic Biology, Department of Bioengineering, Department of Biomedical and Translational Sciences, University of Illinois, 1207 West Gregory Drive, Urbana, Illinois, 61801, USA; Fax: 2173338286; Tel: 2173332239; E-mail: mbwheele@illinois.edu

Calcium Phosphate Treatment Enhances Osteogenic Differentiation of Porcine Adipose-Derived Stem Cells on Fibrin Scaffolds

2

Potential methods to increase blood clot stiffness include reducing red blood cells, porosity, and pH, and adding stiff granules to form a composite. Reducing pH increases the protonation of residues, resulting in more charged inter-helical interactions. Creating composites with more rigid, insoluble materials such as calcium phosphates, could result in more balanced properties, similar to the collagen-hydroxyapatite composite of bone [5]. Highly-deformable red blood cells, designed to move flexibly through capillaries, decrease the stiffness of blood clots due to their low stiffness (order of 10 Pa) [6]. Therefore, reducing the number and intactness of red blood cells in a blood clot may increase stiffness. In addition, the crosslinking density of fibrin is below its maximum [7]. Finally, reducing porous space between fibers significantly increases stiffness [8]. Fibrin is a flexible hydrogel whose polymerization conditions determine its structure and properties, which may be modified for improved bone defect healing.

Several recent studies have examined the use of fibrin or modified fibrin in bone regeneration [9-15]. However, only one study examined the use of autologous fibrin as a scaffold for bone regeneration [10]. That study used the human fibrin scaffolds and viral transduced human muscle-derived stem cells (hMDSC) in a rat calvarial model to examine bone regeneration. Furthermore, these recent studies did not examine methods or treatments to increase the stiffness of the autologous fibrin scaffolds before culture and differentiation of the stem cells. This study was designed to develop a fibrin scaffold for optimum *in vitro* osteogenic differentiation of porcine ASCs as a model system for human bone regeneration.

Materials And Methods

I Blood Collection and Fibrin Modification

Whole blood was collected in sterile 1-liter containers from 6 pigs and allowed to clot with different treatments, which included solutions (2.4 and 7.2 mM) of calcium chloride ($CaCl_2$, Sigma C7902), or calcium hydrogen phosphate ($CaHPO_4$, Mallinckrodt #4272), a precursor to bone mineral (hydroxyapatite, $Ca_5(PO_4)_3OH$). Highly flexible red blood cells (RBCs) were removed osmotically with red blood cell lysis buffer (25% or 50% to blood, 8.3 g/L ammonium chloride, Sigma R7757). Fibrin scaffolds were mechanically compressed under pressure (200 MPa) to reduce porosity in a syringe using free weights or placed under vacuum (130 kPa) during coagulation and stored at -20°C [16].

II Coagulation Time

During whole blood collection, samples from 4 pigs were timed to determine the coagulation rate under various treatments. Blood was collected in 50 mL centrifuge tubes and agitated manually. Timing began upon collection in an individual centrifuge tube and ended upon cessation of motion during tube rocking [17]. Coagulation time was normalized to untreated whole blood for each pig.

III *In Vitro* Degradation

Fibrin scaffolds were cut into approximately 2-gram sections and pressed flat onto 10 cm² tissue culture plates with 5 mL of Dulbecco's Modified Eagle's Medium (DMEM) with varying concentrations (0, 1, 5, 10%) of fetal bovine serum (FBS) [18]. At weekly intervals, samples were digitally scanned to observe degradation. The surface area of each scaffold was calculated using an image analysis programme (ImageJ, National Institutes of Health, Bethesda, MA). The area was normalized by its original value (day 0) to calculate the percent change in the area. Samples were fixed in 10% formalin.

Microstructural changes were compared using scanning electron microscopy (SEM). Samples were dehydrated in an increasing ethanol series and stored in a desiccation chamber overnight. Samples were then critical point dried using liquid carbon dioxide. After applying a 50 mbar vacuum and inducing eccentric rotation, samples were sputter coated with gold-palladium (Au-Pd) for 45 seconds [19]. Samples were imaged using a Phillips XL30 (FEI Company) SEM. The beam voltage was 10 kV with a spot size of 5. Images were recorded at 500x magnification.

IV Mechanical Testing

Test specimens were prepared as right circular cylinders 25 mm in diameter and 30 mm in height for mechanical testing (Instron Model 5567) [20]. A compression test at constant velocity (1 mm/min) was performed on hydrated samples (n = 5). Original dimensions were used to calculate stress and strain, and resulting curves were used to determine elastic modulus. Analysis was limited to the initial linear region of 10% strain [21]. Cylindrical samples of 1 cm diameter and 1 cm height were prepared in centrifuge tube caps for nanoindentation (n = 4). A TI950 hysitron tribometer, using a 90° conical PMMA tip, was used to indent samples 10 µm in depth to determine relative sample stiffness. Stiffness was calculated as the slope of the tip removal curve between 40-90% displacement [22].

V Adipose-Derived Stem Cell Co-Culture and Osteogenic Differentiation

Fibrin scaffolds were thawed and sectioned (1 mm thickness). Sections were sterilized using ethylene oxide gas exposure overnight before washing them with phosphate-buffered saline (PBS). Scaffolds were placed in tissue culture plates and cultured overnight under standard conditions before the addition of passage 2-3 ASCs (1×10^5 cells per cm²), which were previously isolated from a pig transgenic for green fluorescent protein (GFP) [23]. ASCs were cultured in DMEM with 10% FBS incubated with 5% carbon dioxide at 39°C. Cell attachment to fibrin was observed with a fluorescent microscope.

At 80% confluence, media was supplemented with 10 mM β-glycerophosphate, 50 µM ascorbic acid, and 1 µM dexamethasone to induce osteogenic differentiation [24]. Cells were cultured for 0, 14, and 28 days before fixation in 10% formalin. Osteogenic differentiation of ASC resulted in the formation of circular nodules. The nodules were imaged using a fluorescent microscope (Nikon Diaphot-TMD) and digital camera. After fluorescent imaging, the average area per nodule (n = 30) was quantified using ImageJ (National Institutes of Health, Bethesda, MA). The average nodule radius was calculated assuming a circular nodule, using the equation [24]:

Radius = sqrt(Area / π)

VI Statistical Analysis

Quantitative data are presented as mean ± standard error. One-way analysis of variance (ANOVA) was performed using SAS statistical analysis software (SAS Institute, Cary, NC). Fisher's exact test was used for pairwise mean comparisons. A total of 3 scaffolds per treatment per timepoint (n = 3) were analysed for a total of 18 scaffolds (n = 18) and 30 nodules per treatment per timepoint (n = 30). Significance was evaluated using an alpha level of 0.05.

Results

I Coagulation Time

The average coagulation time of untreated whole blood was 121 seconds. Treatment with calcium phosphate reduced coagulation time by 25% but was not different from that of whole blood. Treatment with red blood cell lysis buffer significantly increased clotting time by 80% over calcium phosphate treatment (p<0.05) and by 35% over whole blood (p<0.1). Following normalization, differences between all three treatments were statistically significant (p<0.05; Figure 1). Coagulation times of calcium chloride treatments could not be assessed due to low stiffness, as samples remained in motion during manual agitation even after coagulation was complete.
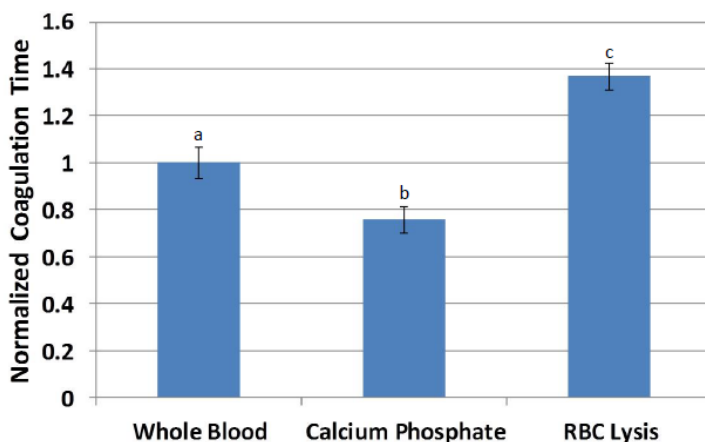

Figure 1: Coagulation time of blood normalized relative to untreated whole blood for each pig. [a,b,c] Treatments with different superscripts differ (p<0.05).

II *In Vitro* Degradation

Evidence of bulk degradation was present in most treatments (Figure 2). In addition, increasing fetal bovine serum concentration generally resulted in a higher amount of degradation. Control blood clots had 98% remaining after 28 days in culture with serum-free DMEM (0% FBS) and 80% remaining after culture in DMEM with 10% FBS. Clots treated with calcium chloride were more resistant to degradation (92%

remaining, p = 0.097) compared to whole blood, while clots treated with red blood cell lysis buffer were less resistant (74% remaining, p = 0.14) compared to whole blood after 28 days in culture with 10% FBS (Figure 3). Degradation percentages between whole blood, vacuum-treated and calcium phosphate-treated blood were not significantly different. However, degradation percentage of calcium chloride-treated blood was significantly less (p<0.05) than that of RBC lysis buffer-treated blood, but neither one of these were different from the other 3 treatments.
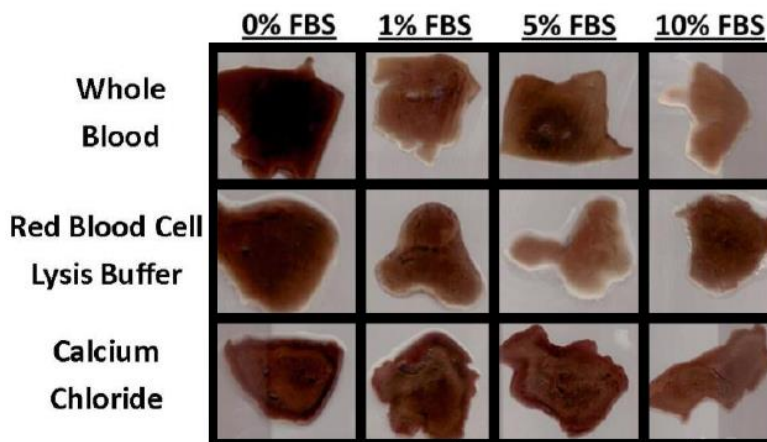

Figure 2: Representative 2-D cross-sections of fibrin scaffolds after 28 days in culture. The presence of FBS increased the rate of degradation, which varied depending on scaffold treatment.
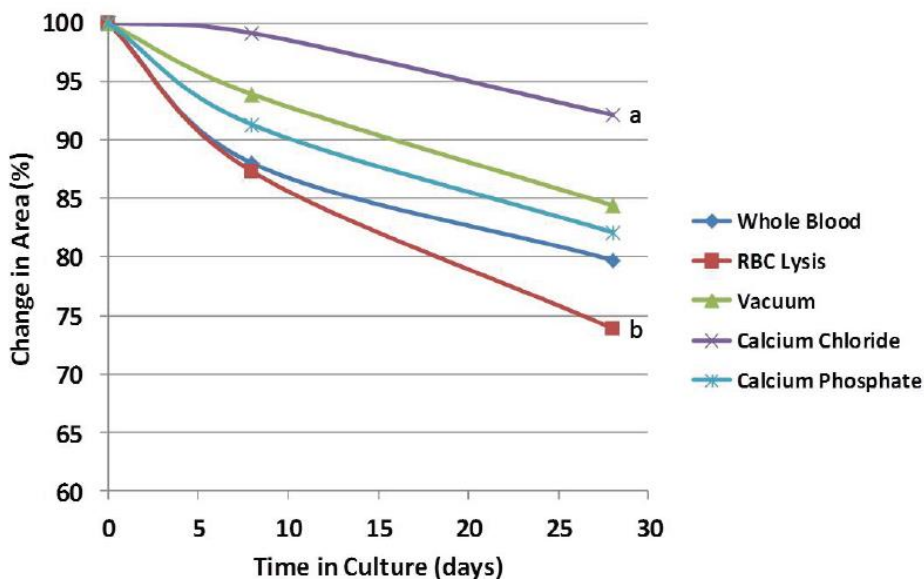
Figure 3: Relative change in the cross-sectional area during culture in 10% fetal bovine serum. Scaffold treatment affected the degradation rate, but treatments remained relatively stable over the timeframe of osteogenic differentiation (28 days). [a,b] Treatments with different superscripts differ ($p < 0.05$).

Analysis of scaffolds using SEM (Figure 4) displayed little structural differences for whole blood, calcium chloride, and red blood cell lysis buffer treatments. Calcium phosphate treatment resulted in a more granular surface with notable roughness whereas vacuum and compression-treated scaffolds appeared smoother.
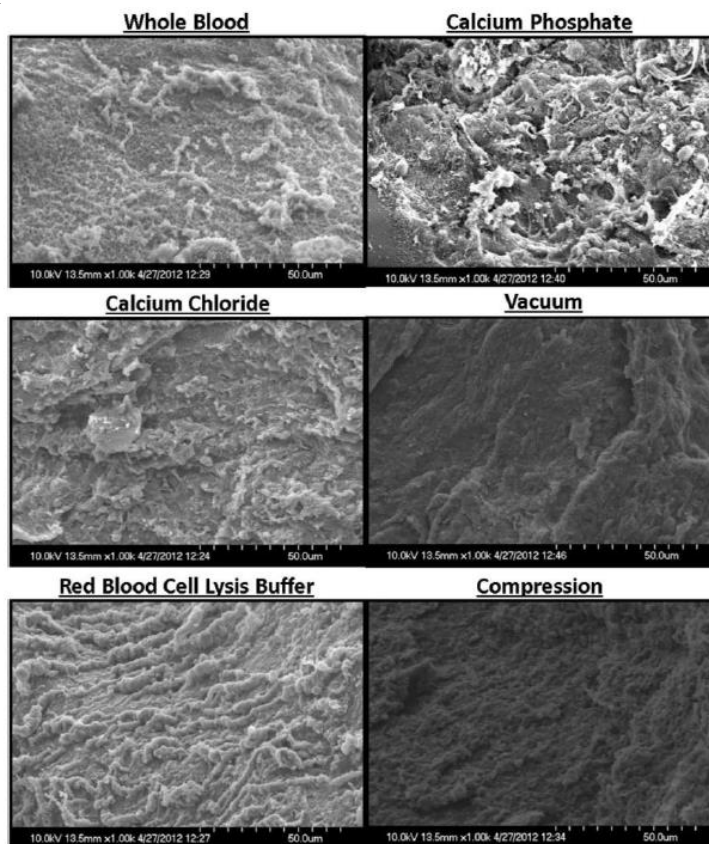

Figure 4: Representative SEM images of fibrin scaffolds. While whole blood, calcium chloride, and red blood cell lysis buffer scaffolds displayed little differences in structure, calcium phosphate treatment resulted in a more granular surface with notable roughness. Vacuum and compression-treated scaffolds appeared smoother.

III Mechanical Testing

Measured by compression testing, the average elastic modulus of fibrin scaffolds (Figure 5) derived from whole blood was 1.9 kPa. Scaffolds treate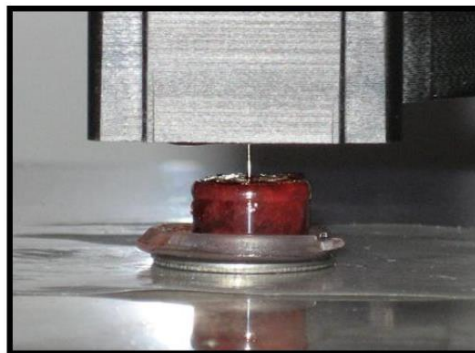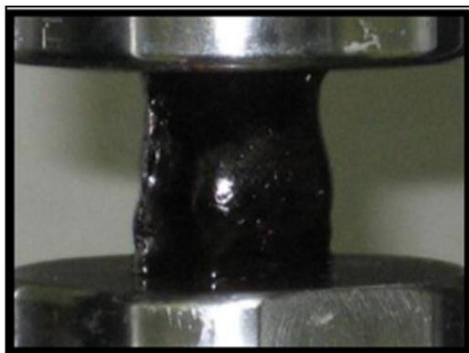d with RBC lysis buffer were higher in stiffness by 25% (p = 0.092). In addition, scaffolds treated with $CaHPO_4$ had a similar higher stiffness (p = 0.089). Scaffolds coagulated under vacuum or mechanical compression showed no change in stiffness compared to whole blood. Treatment with $CaCl_2$ significantly reduced stiffness by 37% (p = 0.025, Figure 6) compared to whole blood.
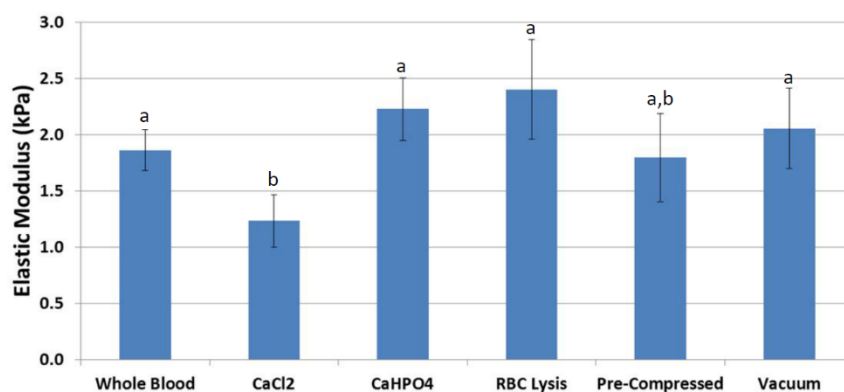

Figure 5: Experimental setups for compression testing (left) included preparing right circular cylinders 25 mm in diameter and 30 mm in height and compressing samples using an instron model 5567. Calculated stresses and strains were used to determine elastic modulus. Nanoindentation (right) used samples 1 cm in diameter and 1 cm in height. Samples were indented using a 90° conical PMMA tip, indenting 10 μm depth. Stiffness was calculated as the slope of the tip removal curve between 40-90% strain.

Figure 6: Compression testing results displayed higher stiffness in scaffolds treated with RBC lysis buffer and calcium hydrogen phosphate. Scaffolds coagulated under vacuum or mechanical compression showed little difference, and scaffolds treated with calcium chloride had lower stiffness. [a,b] Treatments with different superscripts differ (p ≤ 0.025).

Nanoindentation (Figure 7) stiffness measurements were significantly higher for scaffolds treated with calcium phosphate (average 94 kPa, p = 0.00024) compared to that of whole blood (47 kPa). Stiffness measurements of scaffolds treated with red blood cell lysis buffer were also higher than that of whole blood (p = 0.095). Normalization by individual pig (Figure 8) resulted in stiffness nearly two times higher for calcium phosphate (p = 0.0053) and a trend higher for red blood cell lysis buffer (p = 0.064). Scaffolds from other treatments could not be accurately measured due to low stiffness.
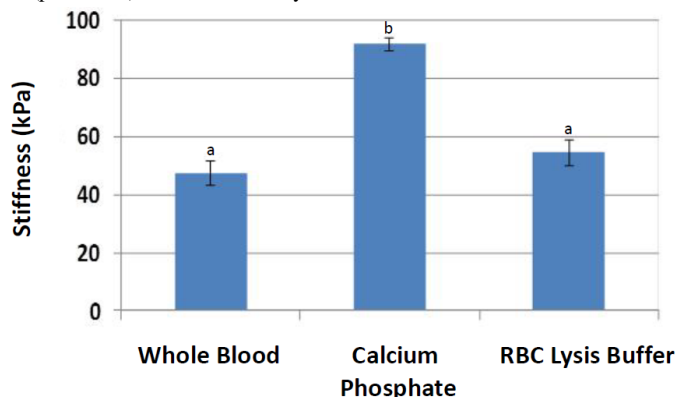

Figure 7: Nanoindentation results were significantly higher in stiffness for scaffolds treated with calcium phosphate. Scaffolds treated with red blood cell lysis buffer trended higher (p<0.1) compared to whole blood. [a, b] Treatments with different superscripts differ (p<0.05).
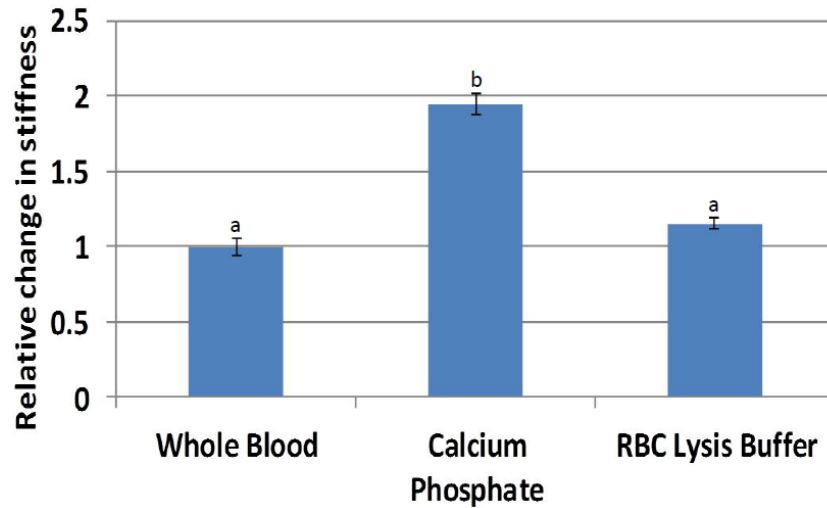
Figure 8: Stiffness normalized by individual pig were significantly higher in stiffness for scaffolds treated with calcium phosphate. Scaffolds treated with red blood cell lysis buffer trended higher (p<0.1) compared to whole blood.

[a,b] Treatments with different superscripts differ (p<0.05).

IV Osteogenic Differentiation

GFP-ASCs attached to fibrin within two days and differentiated into an osteogenic phenotype when cultured in media supplemented with dexamethasone, β-glycerophosphate, and ascorbic acid (Figure 9). Over time, bone-like nodules formed, which were observed using fluorescent microscopy. Osteogenic nodules were observed by seven days and increased in density until 14 days. Nodules increased in size through 21 days, then appeared to grow at a slower pace until 28 days. The average area (Figure 10) and average radius (Figure 11) per nodule were lower on fibrin scaffolds derived from whole blood compared to control polystyrene (tissue culture plastic, p = 0.029). However, nodules on fibrin scaffolds treated with calcium phosphate were larger than control whole blood (p = 0.042).
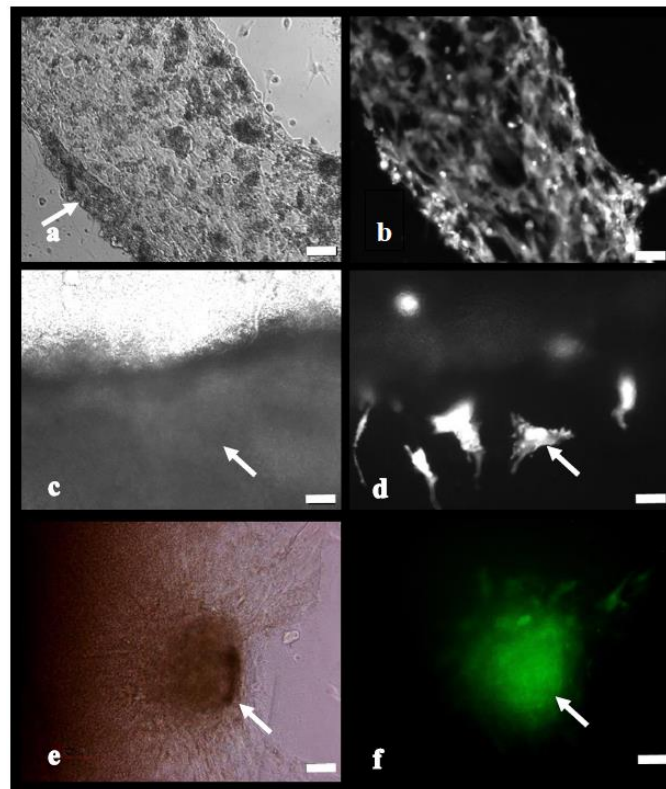

Figure 9: Paired phase contrast and fluorescent images of ASCs (white arrows) expressing green fluorescent protein attaching to (a, b and c, d) and differentiating (e, f) on fibrin scaffolds. Scale a and b - 25 μm. Scale c and d - 50 μm. Scale e and f - 100 μm.
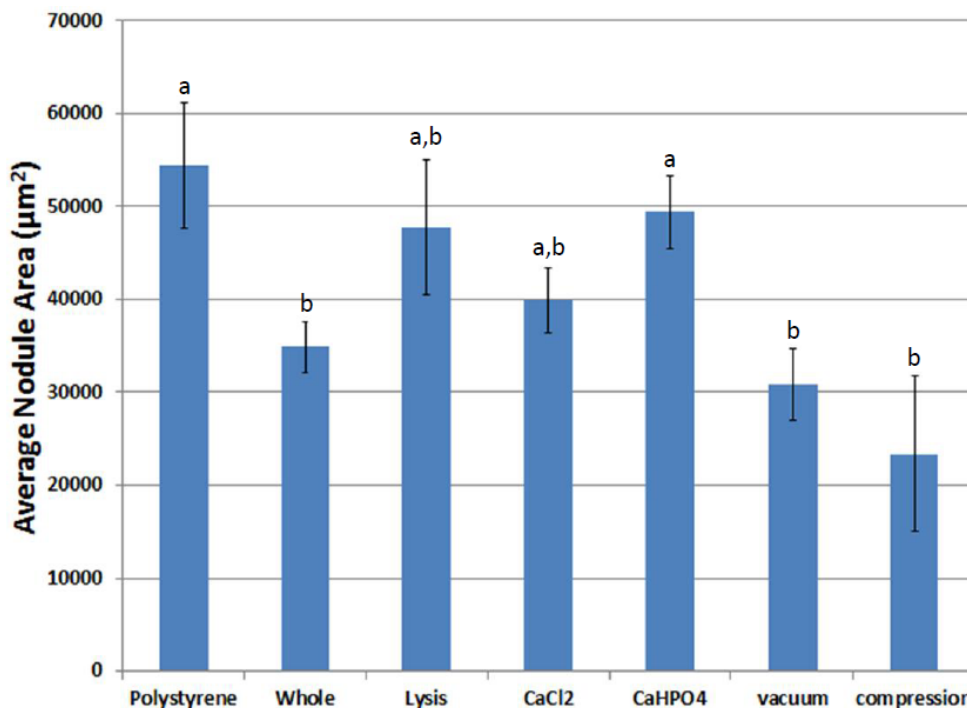
Figure 10: Average nodule area during osteogenic differentiation on scaffolds of various treatments. [a,b] Treatments with different superscripts significantly differ ($p < 0.05$).
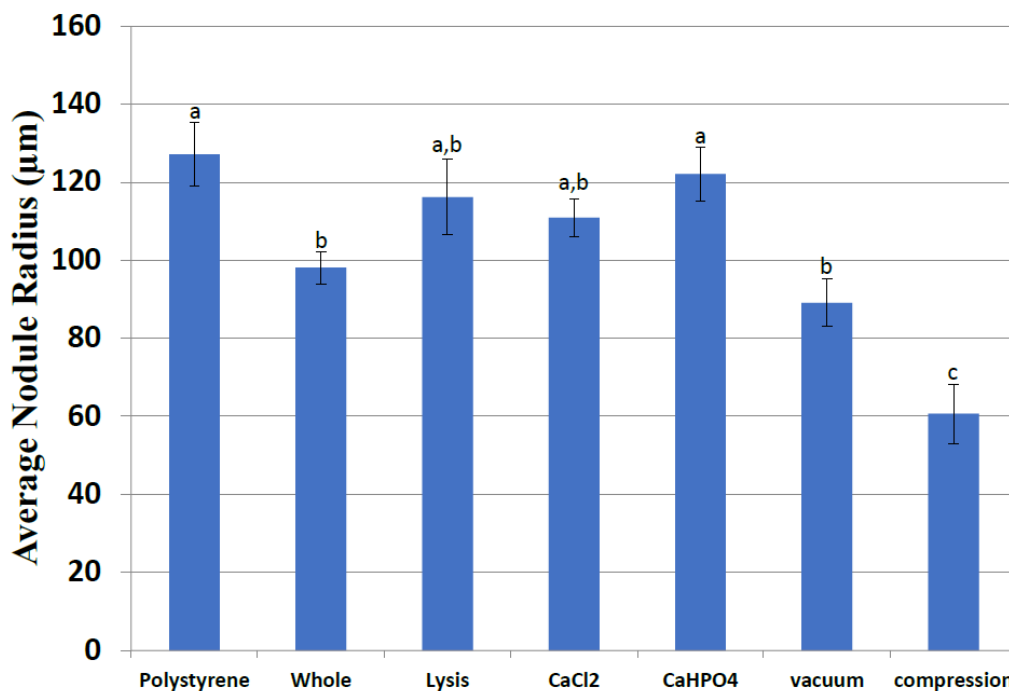
Figure 11: Average nodule radius during osteogenic differentiation on scaffolds of various treatments. [a,b,c] Treatments with different superscripts significantly differ ($p < 0.05$).

Discussion

The primary objective of these experiments was to develop an optimal preparation of whole blood-derived fibrin scaffold, which was practical, biocompatible, and osteoconductive. Based on the results, fibrin supplemented with granules of calcium hydrogen phosphate ($CaHPO_4$) was determined to be the most suitable formulation of those examined. Using calcium phosphate resulted in a fibrin scaffold that coagulated faster ($p = 0.022$), had a rougher surface, and higher stiffness, desirable properties for practical use during surgical operations and scaffolds used

in bone tissue engineering. Further, $CaHPO_4$ treatment enhanced osteogenic differentiation on fibrin scaffolds compared to untreated control whole blood.

Calcium phosphates and calcium chlorides act as natural pro-coagulants due to increased concentrations of soluble calcium ions, an essential element for activating both factor X and thrombin in the coagulation cascade [1]. However, these ionic compounds are on different extremes of the solubility scale, with $CaCl_2$ being highly soluble in water while $CaHPO_4$ being minimally soluble in water. Differences in solubility affect the bioavailability of calcium ions and thus modify their effect during fibrin polymerization. From calcium chloride, the increased soluble calcium ion concentration likely allows for more simultaneous initiation sites of fibrin polymerization, resulting in a scaffold that gels more rapidly with lower average chain length which likely explains the poor stiffness displayed by the $CaCl_2$ treated fibrin scaffolds [25].

For calcium phosphate, this effect is mitigated by fewer available calcium ions, while providing relatively insoluble nucleation sites for initiating and stabilizing fibrin polymerization. Initial contact activation is the most prolonged phase of the coagulation process [17]. Adding calcium phosphate granules significantly increases the available surface area for contact activation and is likely to account for the observed reduction in coagulation time with calcium phosphate. In addition, the concentration of fibrinogen also has an essential effect on coagulation, with lower concentrations resulting in fibrin gels that polymerize slower. Dilution of fibrinogen and other coagulation factors by red blood cell lysis buffer likely explains its slower coagulation time.

For both *in vitro* and *in vivo* environments, fibrinolysis proceeds through two related mechanisms, bulk and enzymatic degradation [26]. Bulk degradation results from water infiltration and hydrolysis, reducing chain lengths and network connectivity [27]. Enzymatic degradation proceeds primarily through the enzyme plasmin, which circulates in an inactive form in the blood and is present in fetal bovine serum [26]. Adding FBS to culture media increased fibrinolysis regardless of treatment, indicating the significant role of enzymatic degradation, while bulk degradation was slower in comparison.

Fibrin scaffolds treated with calcium chloride or coagulated under vacuum showed notable degradation reductions (higher area remaining) compared to fibrin scaffolds derived from whole blood. Though multiple mechanisms may determine this result, the chemical property of a shorter average chain length is likely to be a dominant factor for calcium chloride treatment [28]. However, for vacuum coagulation, the physical property of reduced porosity aids in reducing water infiltration and surface exposure to plasmin, slowing both bulk and enzymatic degradation [29]. In contrast, scaffolds treated with red blood cell lysis buffer likely had increased water infiltration and plasmin exposure due to the osmotic dissolution of red blood cells, resulting in higher (p = 0.097) degradation (lower area remaining) compared to controls.

A rough surface is generally preferable to a smooth surface for attachment-dependent cell types such as adipose-derived stem cells [30]. Surface roughness provides more opportunities for multidirectional cell attachments, more similar to that experienced by cells *in vivo*, and

increased surface area for attachment and material transport. For fibrin scaffolds, roughness is primarily due to red blood cells (7 μm average diameter). Red blood cells likely account for the surface roughness viewable by scanning electron microscopy for untreated whole blood scaffolds and calcium chloride-treated scaffolds. In contrast, the osmotic destruction of red blood cells by red blood cell lysis buffer may explain the slight increase in surface roughness. However, ASCs generally do not directly attach to red blood cells. In contrast, attachment-dependent cell types can be attached to calcium phosphate granules, which have granule sizes on a similar scale [31]. The addition of granules appears to provide increased surface roughness to fibrin scaffolds. Using vacuum or mechanical compression may flatten red blood cells, causing fibrin to appear smoother.

In addition, adipose-derived stem cells, among other fibroblast-like cell types, are not known to maintain receptors for direct attachment to fibrin. Therefore, cell attachment is likely to proceed through intermediates such as fibronectin, which circulates in blood along with fibrinogen and becomes entrapped within the developing blood clot during coagulation [32, 33]. Reduced direct attachment to fibrin may help explain, in part, the limited success of using fibrin-only glues for tissue regeneration. ASCs appeared to attach and differentiate on whole blood-derived fibrin scaffolds. Fibrin scaffolds derived from whole blood maintain several advantages over those prepared from only fibrinogen and thrombin. These include the simple and inexpensive collection and retaining of essential blood constituents in the wound healing process, such as fibronectin and platelet aggregates [34]. However, the use of whole blood-derived fibrin comes at the cost of reduced operative control of fibrin polymerization and reduced clot stiffness due to the presence of red blood cells.

As measured by compression testing, the bulk stiffness of fibrin scaffolds did not appreciably increase from a practical standpoint regardless of treatment and remained several orders of magnitude lower than trabecular bone [3]. However, microscale stiffness, as measured by nanoindentation, significantly increased with calcium phosphate treatment compared to controls. The effect of calcium phosphate may be related to its inherently high stiffness as a ceramic as well as the potential of its granules to act as anchors for the fibrin network. The mechanical properties of fibrin-calcium phosphate composites can be approximated as a weighted average of the two substances [35]. Increased stiffness at the microscale has been demonstrated to favour osteogenic differentiation of adipose-derived stem cells, whereas softer surfaces favour other cell types such as neurons and myocytes [36]. The mechanisms for this phenomenon are under investigation but are related to the interdependent relationship between mechanical forces on the extracellular matrix and gene expression.

A difference in measured stiffness values of approximately one order of magnitude was observed between the methods of compression testing and nanoindentation. These results are likely explained by the hydrated, physiological testing conditions and the role of water in fibrin viscoelasticity [37]. Surface tension is a much more dominant force in nanoindentation measurements. Water can flow more freely under a bulk compression testing regimen, which may reduce observed elastic (storage) modulus. Applying sinusoidal stress, used in methods such as

Calcium Phosphate Treatment Enhances Osteogenic Differentiation of Porcine Adipose-Derived Stem Cells on Fibrin Scaffolds

9

dynamic mechanical analysis, could rectify this difference in observed values and better account for the viscoelastic behaviour of fibrin scaffolds, which are similar to hydrogel polymers [38].

Regarding osteoconductivity, one notable result is the tendency of ASCs to form larger nodules on tissue culture plastic (irradiated polystyrene) compared to whole blood-derived fibrin. This result is likely partly explained by methods used in ASC isolation, including the expansion of cells that adhere onto tissue culture plastic [24]. While starting as a heterogeneous cell population, the cells which attach and divide most rapidly dominate in number [39]. Therefore, ASC isolation methods introduce a strong selection for attachment to polystyrene.

Conclusion

The ability of ASCs to attach and migrate towards each other is essential for the formation of osteogenic nodules over a timescale of weeks. The potential factors of improved cell attachment, presence of calcium and phosphate ions, surface roughness, and increased stiffness on the microscale may each play a role in the increase in osteoconductivity of ASCs for fibrin treatments of red blood cell lysis buffer, calcium chloride, and calcium phosphate, as measured by histomorphometry. Treatment of fibrin scaffolds with calcium phosphate appears to improve each of these characteristics *in vitro*. Therefore, *in vivo* experiments are warranted in the future to test if CaHPO$_4$-treated fibrin scaffolds will demonstrate similar characteristics in live animals.

REFERENCES

1. Davie EW, Fujikawa K, Kisiel W (1991) The coagulation cascade: initiation, maintenance, and regulation. *Biochemistry* 30: 10363-10370. [Crossref]

2. Shen LL, Hermans J, McDonagh J, McDonagh RP, Carr M (1975) Effects of calcium ion and covalent crosslinking on formation and elasticity of fibrin gels. *Thromb Res* 6: 255-265. [Crossref]

3. Ashman RB, Rho JY (1988) Elastic modulus of trabecular bone material. *J Biomech* 21: 177-181. [Crossref]

4. Maeno S, Niki Y, Matsumoto H, Morioka H, Yatabe T et al. (2005) The effect of calcium ion concentration on osteoblast viability, proliferation and differentiation in monolayer and 3D culture. *Biomaterials* 26: 4847-4855. [Crossref]

5. Le Nihouannen D, Saffarzadeh A, Gauthier O, Moreau F, Pilet P et al. (2008) Bone tissue formation in sheep muscles induced by a biphasic calcium phosphate ceramic and fibrin glue composite. *J Mater Sci Mater Med* 19: 667-675. [Crossref]

6. Dao M, Lim CT, Suresh S (2003) Mechanics of the human red blood cell deformed by optical tweezers. *Journal of the Mechanics and Physics of Solids* 51: 2259-2280.

7. Lewis KB, Teller DC, Fry J, Lasser GW, Bishop PD (1997) Crosslinking Kinetics of the Human Transglutaminase, Factor XIII[A2], Acting on Fibrin Gels and γ-Chain Peptides. *Biochemistry* 36: 995-1002. [Crossref]

8. Duong H, Wu B, Tawil B (2009) Modulation of 3D Fibrin Matrix Stiffness by Intrinsic Fibrinogen-Thrombin Compositions and by Extrinsic Cellular Activity. *Tissue Eng Part A* 15: 1865-1876. [Crossref]

9. Noori A, Ashrafi SJ, Vaez Ghaemi R, Hatamian Zaremi A, Webster TJ (2017) A review of fibrin and fibrin composites for bone tissue engineering. *Int J Nanomedicin* 12: 4937-4961 [Crossref]

10. Gao X, Cheng H, Sun X, Lu A, Ruzbarsky JJ et al. (2021) Comparison of Autologous Blood Clots with Fibrin Sealant as Scaffolds for Promoting Human Muscle-Derived Stem Cell-Mediated Bone Regeneration. *Biomedicines* 9: 983. [Crossref]

11. Shi W, Que Y, Zhang X, Bian L, Yu X et al. (2021) Functional tissue-engineered bone-like graft made of a fibrin scaffold and TG2 gene-modified EMSCs for bone defect repair. *NPG Asia Mater* 13: 28.

12. Cassaro CV, Justulin Jr LA, de Lima PR, de Assis Golim M, Biscola NP et al. (2019) Fibrin biopolymer as scaffold candidate to treat bone defects in rats. *J Venom Anim Toxins Incl Trop Dis* 25: e20190027. [Crossref]

13. Creste CFZ, Orsi PR, Landim Alvarenga FC, Justulin LA, de Assis Golim M et al. (2020) Highly effective fibrin biopolymer scaffold for stem cells upgrading bone regeneration. *Materials (Basel)* 13: 2747. [Crossref]

14. Pathmanapan S, Periyathambi P, Anandasadagopan SK (2020) Fibrin hydrogel incorporated with graphene oxide functionalized nanocomposite scaffolds for bone repair - In vitro and in vivo study. *Nanomedicine* 29: 102251. [Crossref]

15. Shi W, Bian L, Wu Y, Wang Z, Dai Y et al. (2022) Enhanced Bone Regeneration Using a ZIF-8-Loaded Fibrin Composite Scaffold. *Macromol Biosci* 22: e2100416. [Crossref]

16. Pieters M, Jerling JC, Weisel JW (2002) Effect of freeze-drying, freezing and frozen storage of blood plasma on fibrin network characteristics. *Thromb Res* 107: 263-269 [Crossref]

17. Hattersley PG (1966) Activated coagulation time of whole blood. *JAMA* 196: 436-440. [Crossref]

18. Marder VJ, Francis CW (1983) Plasmin Degradation of Cross-Linked Fibrin. *Ann N Y Acad Sci* 408: 397-406 [Crossref]

19. Le Nihouannen D, Le Guehennec L, Rouillom T, Pilet P, Bilban M et al. (2006) Micro-architecture of calcium phosphate granules and fibrin glue composites for bone tissue engineering. *Biomaterials* 27: 2716-2722. [Crossref]

20. Johnson B, Bauer JM, Niedermajer DJ, Crone WC, Beebe DJ (2004) Experimental techniques for mechanical characterization of hydrogels at the microscale. *Experimental Mechanics* 44: 21-28.

21. Kong HJ, Lee KY, Mooney DJ (2002) Decoupling the dependence of rheological/mechanical properties of hydrogels from solids concentration. *Polymer* 43: 6239-6246.

22. Oyen ML (2017) Nanoindentation of biological and biomimetic materials. *Experimental Techniques* 37: 73-87.

23. Liu ZH, Song J, Wang Z, Tian JT, Kong QR et al. (2008) Green fluorescent protein (GFP) transgenic pig produced by somatic cell nuclear transfer. *Chinese Science Bulletin* 53: 1035-1039.

24. Monaco E, de Lima AS, Bianaz M, Maki A, Wilson SM et al. (2009) Morphological and transcriptomic comparison of adipose and bone marrow derived porcine stem cells. *The Open Tissue Engineering and Regenerative Medicine Journal* 2: 20-33.

25. Boyer MH, Shainoff JR, Ratnoff OD (1972) Acceleration of fibrin polymerization by calcium ions. *Blood* 39: 382-387. [Crossref]

26. Wiman B, Collen D (1978) Molecular mechanism of physiological fibrinolysis. *Nature* 272: 549-550. [Crossref]

27. Göpferich A (1997) Polymer Bulk Erosion. *Macromolecules* 30: 2598-2604.

28. Blombăck B, Hogg DH, Gardlund B, Hessel B, Bohdan K (1976) Fibrinogen and fibrin formation. *Thrombosis Research* 8: 329-346.

29. Kolev K, Tenekedjiev K, Komorowicz, Machovich R (1997) Functional evaluation of the structural features of proteases and their substrate in fibrin surface degradation. *J Biol Chem* 272: 13666-13675. [Crossref]

30. Lampin M, Clerout W, Legris C, Degrange M, Sigot Luizard MF (1997) Correlation between substratum roughness and wettability, cell adhesion, and cell migration. *J Biomed Mater Res* 36: 99-108. [Crossref]

31. Deligianni DD, Katsala ND, Koutsoukos PG, Missirlis YF (2001) Effect of surface roughness of hydroxyapatite on human bone marrow cell adhesion, proliferation, differentiation and detachment strength. *Biomaterials* 22: 87-96. [Crossref]

32. Clark RA, Lanigan DellaPelle P, Manseau E, Dvorak HF et al. (1982) Fibronectin and fibrin provide a provisional matrix for epidermal cell migration during wound reepithelialization. *J Invest Dermatol* 79: 264-269. [Crossref]

33. Proctor RA (1987) Fibronectin: A Brief Overview of Its Structure, Function, and Physiology. *Rev Infect Dis* 9 Suppl 4): S317-S321. [Crossref]

34. Rand MD, Lock JB, Veer CV, Gaffney DP, Mann KG (1996) Blood clotting in minimally altered whole blood. *Blood* 88: 3432-3445. [Crossref]

35. Mooney RG, Costales CA, Freeman EG, Curtin JM, Corrin AA et al. (2006) Indentation micromechanics of three-dimensional fibrin/collagen biomaterial scaffolds. *Journal of Materials Research* 21: 2023-2034.

36. Engler AJ, Sen S, Sweeney HL, Discher DE (2006) Matrix Elasticity Directs Stem Cell Lineage Specification. *Cell* 126: 677-689. [Crossref]

37. Fukada E, Kaibara M (1976) Rheological measurements of fibrin gels during clotting. *Thromb Res* 8: 49-58. [Crossref]

38. Weisel JW (2004) The mechanical properties of fibrin for basic scientists and clinicians. *Biophys Chem* 112: 267-276. [Crossref]

39. Oedayrajsingh-Varma MJ, van Ham SM, Knippenberg M, Helder MN, Klein Nulend J et al. (2006) Adipose tissue-derived mesenchymal stem cell yield and growth characteristics are affected by the tissue-harvesting procedure. *Cytotherapy* 8: 166-177. [Crossref]